Homo- and Heterotypic Cell Contacts in Malignant Melanoma Cells and Desmoglein 2 as a Novel Solitary Surface Glycoprotein

Christian J. Schmitt[1,2], Werner W. Franke[2], Sergij Goerdt[1], Berit Falkowska-Hansen[3], Steffen Rickelt[2] and Wiebke K. Peitsch[1,2]

During progression of melanomas, a crucial role has been attributed to alterations of cell–cell adhesions, specifically, to a "cadherin switch" from E- to N-cadherin (cad). We have examined the adhesion of melanoma cells to each other and to keratinocytes. When different human melanoma cell lines were studied by protein analysis and immunofluorescence microscopy, six of eight lines contained N-cad, three E-cad, and five P-cad, and some lines had more than one cad. Surprisingly, two N-cad-positive lines, MeWo and C32, also contained desmoglein 2 (Dsg2), a desmosomal cad previously not reported for melanomas, whereas other desmosome-specific proteins were absent. This finding was confirmed by reverse transcriptase–PCR, immunoprecipitation, and matrix-assisted laser desorption ionization–time of flight analyses. Double-label confocal and immunoelectron microscopy showed N-cad, α- and β-catenin in plaque-bearing puncta adhaerentia, whereas Dsg2 was distributed rather diffusely over the cell surface. In cocultures with HaCaT keratinocytes Dsg2 was found in heterotypic cell contact regions. Correspondingly, immunohistochemistry revealed Dsg2 in five of 10 melanoma metastases. Together, we show that melanoma cell adhesions are more heterogeneous than expected and that certain cells devoid of desmosomes contain Dsg2 in a non-junction-restricted form. Future studies will have to clarify the diagnostic and prognostic significance of these different adhesion protein subtypes.

Journal of Investigative Dermatology (2007) **127,** 2191–2206; doi:10.1038/sj.jid.5700849; published online 10 May 2007

INTRODUCTION

Under physiological conditions, melanocytes and keratinocytes form the ''epidermal melanin unit'' of the epidermis. Melanocytes are located in the basal layer, in a life-long stable ratio of 1:5 with basal keratinocytes. Dysregulation of this homeostasis may lead to uncontrolled proliferation of the melanocytes and, ultimately, to the development of malignant melanoma (MM). The exact molecular mechanism of this dysregulation is unknown, but an important role has been attributed to alterations in cell–cell communication and adhesion. For example, it has been reported that, compared with normal melanocytes, melanoma cells produce increased amounts of cell adhesion receptors of the immunoglobulin superfamily, correlated with enhanced tumorigenicity and invasiveness (reviewed by Haass *et al.*, 2005).

A group of special importance involved in development and progression of tumors are the cadherins (cads), calcium-dependent transmembrane glycoproteins mediating intercellular adhesion, mostly by homophilic interactions (see the reviews Duguay *et al.*, 2003; Wheelock and Johnson, 2003). So far, more than 80 members of the larger cad superfamily have been identified, including the classical type I and type II cads, which are components of adhering junctions, the desmosomal cads (desmogleins (Dsgs) 1–4 and desmocollins (Dscs) 1–3; for a recent review, see Getsios *et al.*, 2004), protocadherins, fats, seven-pass transmembrane cads, and Ret tyrosine kinases. The type I cads comprise E-cad, typically synthesized by epithelial cells, N-cad on neuronal and mesenchymal cells, and P-cad, first identified in the placenta, and differ from type II cads by the adhesive HAV domain (for review see Nollet *et al.*, 2000). Cads can mediate both homotypic cell–cell interactions, that is, between cells of the same type and heterotypic adhesions between two different cell types.

In normal epidermis, heterotypic melanocyte–keratinocyte adhesions are formed by E-cad (Tang *et al.*, 1994). However, during development of MM, E-cad often appears to be downregulated and replaced by N-cad (Hsu *et al.*, 1996). This phenomenon, also known as ''cadherin switch'', seems

[1]*Department of Dermatology, Medical Center Mannheim, University of Heidelberg, Mannheim, Germany;* [2]*Division of Cell Biology, German Cancer Research Center, Heidelberg, Germany and* [3]*Genetics of Skin Carcinogenesis, German Cancer Research Center, Heidelberg, Germany*

Correspondence: Dr Wiebke K. Peitsch, Department of Dermatology, Medical Center Mannheim, University of Heidelberg, Theodor-Kutzer-Ufer 1-3, 68135 Mannheim, Germany.
E-mail: wiebke.peitsch@haut.ma.uni-heidelberg.de

Abbreviations: cad, cadherin; cat, catenin; Dsc, desmocollin; Dsg, desmoglein; IP, immunoprecipitation; MM, malignant melanoma; PKP, plakophilin

Received 4 December 2006; revised 9 February 2007; accepted 19 February 2007; published online 10 May 2007

important not only for the pathogenesis of MM, but also for some tumrs of epithelial origin (see the reviews Christofori, 2003; Cavallaro and Christofori, 2004; Haass *et al.*, 2004). According to some authors (Li *et al.*, 2001a), N-cad can promote survival and migration of melanoma cells. For melanoma cells, it has also been reported that re-expression of E-cad might restore keratinocyte-mediated growth control and reverse malignancy (Hsu *et al.*, 2000; Li *et al.*, 2004).

In developmental biology, the differentiation and topogenesis of melanocytes provides remarkable examples of cell migration over long distances as well as of drastic changes of cell character, including pigmentation and cell–cell adhesion (for a ''classic'' review, see Le Douarin, 1984). Thus, in typical adhering junctions the originally dominant N-cad can be accompanied and taken over by E-cad and this may then be reversed during malignant growth (see, e.g., Tepass *et al.*, 2000; Niessen and Gumbiner, 2002; Duguay *et al.*, 2003; Foty and Steinberg, 2005).

According to a predominant working hypothesis in cancer research, the switch from E- to N-cad has several functional implications. First, it provides the melanoma cells with a new adhesive repertoire to interact with new, mostly mesenchymal neighbors such as fibroblasts (Li *et al.*, 2001a), blood vessels, and lymphatic tissues. Moreover, N-cad is also thought to be responsible for the transendothelial migration of melanoma cells (Sandig *et al.*, 1997; Li *et al.*, 2001a; Qi *et al.*, 2005). Second, the ''cadherin switch'' may provide proliferative and pro-migratory signals (Kuphal *et al.*, 2004; Qi *et al.*, 2005, 2006; Kuphal and Bosserhoff, 2006). As to other mechanisms regulating E- and N-cad expression in melanoma, several pathways and cell–cell cross-talk interactions have recently been discussed (Poser *et al.*, 2001; Qian *et al.*, 2004; Robert *et al.*, 2006; Liu *et al.*, 2006; see the review Huber *et al.*, 2005).

Functional implications of the ''cadherin switch'' on melanoma development and progression have been described by the Herlyn group and others, who mostly used *in vitro* cell culture systems, including two- and three-dimensional organotypic cultures as well as animal models (Hsu *et al.*, 2000; Li *et al.*, 2001a; 2004; Liu *et al.*, 2006). Immunohistochemical examinations on MMs and their metastases, however, have indicated that this concept in its purest form cannot be conferred 100% to the situation *in situ*. For example, a proportion of melanoma cells in metastases are still positive for E-cad and negative for N-cad (Danen *et al.*, 1996; Hsu *et al.*, 1996; Silye *et al.*, 1998; Sanders *et al.*, 1999). This has led us to search for further cell adhesion molecules involved, both in melanoma cell cultures, in two- and three-dimensional melanoma–keratinocyte cocultures, and in cryostat sections of melanoma metastases. We have found that the cad repertoire of melanoma cells – even within one cell – can be much more heterogeneous than expected. Moreover, most surprisingly, we made the observation that despite the absence of desmosomes and other desmosomal constituents, a number of melanoma cell lines in culture as well as a proportion of melanoma metastatic cells contain, in addition to classical cads, noticeable amounts of the desmosomal cad, Dsg2, as a widely spread, non-junction-bound transmembrane cell–cell adhesion protein.

RESULTS

Coexistence of classical cads in certain melanoma cells

To elucidate the molecular composition of plaque-bearing junctions in MM cells, we first performed immunocytochemistry on several cultured human melanoma cell lines, using antibodies to classical cads. In general, cells were grown to rather high density, as the confluency of cell cultures is known to affect the expression pattern of cads. In WM35 cells, for example (Figure 1), we found more than 90% of the cells to be intensely positive for N-cad, as expected (Figure 1b, c, e, and f). In addition, ~30% of the cells contained E-cad (Figure 1a, c, h, and i), thus confirming Smalley *et al.* (2005) and ~20% P-cad (Figure 1d, f, g, and i), both enriched at intercellular contacts, like N-cad. As seen by double-label confocal microscopy, these three classical cads often appeared in mutually exclusive patterns, but occasionally also within the same cell, showing at least partly overlapping localization (Figure 1c, f, and i, asterisks). In some cells, we could notice co-occurrence of all three cads. To examine our results with a biochemical identification method, immunoblot analyses were performed, showing specific bands for N-, E-, and P-cad in WM35 cells (Figure 1j, lane 5) as well as coexistence of N- and P-cad in another melanoma cell line, C32 (lane 4). In coimmunoprecipitation (IP) experiments, conducted again with WM35 cell lysates, all three cads were found to coimmunoprecipitate with the adhering junction plaque protein β-catenin (cat) (Figure 1k, lanes 2–4). N- and E-cad as well as N- and P-cad did not coprecipitate (lane 2). Remarkably, however, P-cad was specifically enriched in E-cad immunoprecipitates (lane 3), an observation made with two different solubilization buffers (1% Triton X-100 buffer, Figure 1k, and RIPA buffer; data not shown), suggestive of the existence of heterotypic E- and P-cad complexes.

Detection and biochemical characterization of Dsg2 in specific melanoma cell lines

Our findings on WM35 cells led us to a more detailed analysis of melanoma cell junctions. To this end, immunoblot analyses with diverse antibodies against proteins of adhering junctions, desmosomes, and tight junctions were performed on eight different human melanoma cell lines (Figure 2 and Table 1). Six of these eight lines contained N-cad, three WM35, SK-MEL-2, and Malme-3M, were positive for E-cad. In addition, P-cad was detected in five of eight lines, among those both N-cad- (WM-115, C32, and WM35) and E-cad-positive ones (SK-MEL-2, Malme-3M, and WM35). Line WM-115 also contained, in addition to N- and P-cad, cad 11, a cad typical for mesenchymal stem cells (Simonneau *et al.*, 1995; Wuchter *et al.*, 2007). Together, our analyses show that cad complements of melanoma cells are more heterogeneous than hitherto thought.

When the different melanoma cell lysates were immunoblotted with antibodies against desmosomal proteins (Figure 2; for a survey see Table 1), we detected Dsg2, a desmosomal cad normally synthesized in keratinocytes in the

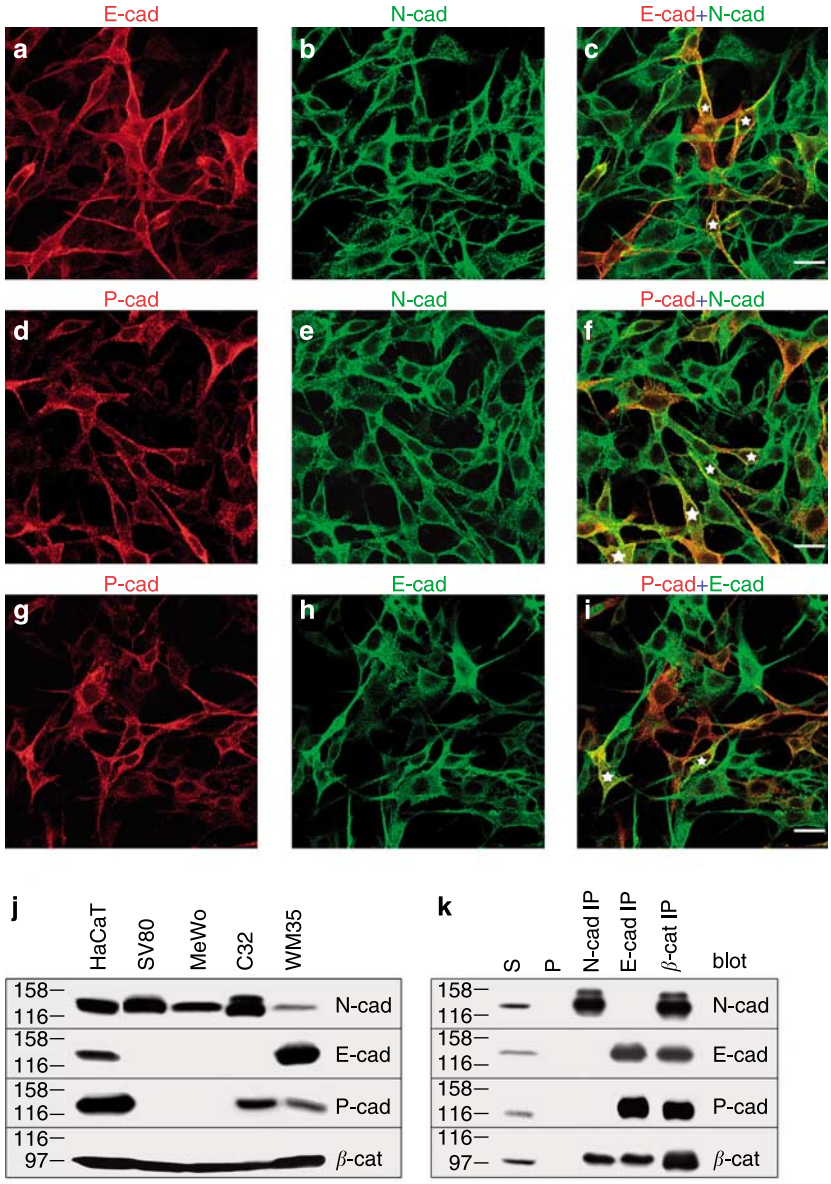

Figure 1. Patterns of coexistence of different classical cads in cultured melanoma cells. (**a**–**i**) Double-label immunofluorescence confocal microscopy of human WM35 melanoma cells using antibodies against N-cad (green in **b**, **c**, **e** and **f**), E-cad (red in **a** and **c**, green in **h** and **i**), and P-cad (red in **d**, **f**, **g**, and **i**), showing that the vast majority of the cells contain N-cad, which appears enriched at intercellular contacts and along cell borders, but also that a minor proportion of the cells is positive for E- and/or P-cad. The different classical cads can sometimes be found in the same cell (asterisks), but occasionally also in mutually exclusive cell patterns (**c**, **f**, and **i**). Bars = 20 μm. (**j**) Immunoblot analysis of the SDS-PAGE-separated polypeptides of total cell lysates from human HaCaT keratinocytes, SV80 fibroblasts, and different human melanoma lines (MeWo, C32 and WM35), confirming the coexistence of more than one classical cad in a given cell line, that is, N- and P-cad in C32 cells and N-, E-, and P-cad in WM35 cells. Equal amounts of proteins have been loaded. (**k**) Immunoblots of the SDS-PAGE-separated proteins of IPs from WM35 cell lysates, using N-, E-, and P-cad as well as β-cat antibodies. Note that N-cad coprecipitates neither with E- nor P-cad, whereas P-cad is pulled down in E-cad immunoprecipitates. S, supernatant before IP; P, material after preclearing. MW markers are indicated on the left margins.

basal epidermal layer, in two of eight melanoma lines, MeWo and C32, an unexpected finding confirmed with three different Dsg2 mAbs (clones DG3.10, 6D8, and 10G11; Figure 2). By contrast, all other desmosomal cads examined, that is, Dsg1 and 3 and Dscs 1–3, were absent. With regard to desmosomal plaque proteins, rather small amounts of plakoglobin, known as a common constituent of both desmosomal and adhering junction plaques (Cowin *et al.*, 1986), were detected in a number of melanoma cell lines, including the Dsg2-positive line C32. Moreover, the other Dsg2-positive line, MeWo, contained plakophilin (PKP) 3 and another line, WM-115, was positive for PKP1, 2, and 3, but negative for desmosomal cads. Interestingly, MeWo cells also synthesized another plaque protein, neurojungin, an arm-repeat protein described previously as a constituent of heterotypic adhering junctions specific for the outer limiting zone of the retina (Paffenholz *et al.*, 1999).

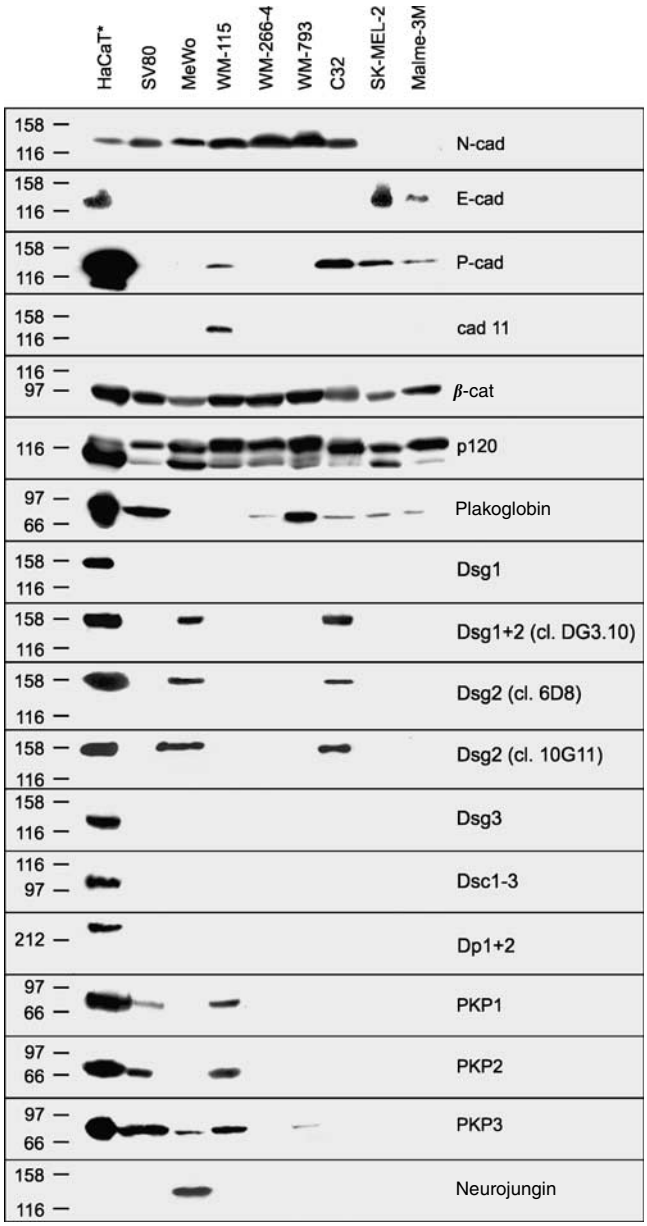

Figure 2. Immunoblot detection of adhering junction-associated and desmosomal proteins in different cultured human melanoma cell lines. Equal amounts of total proteins from seven human melanoma lines (MeWo, WM-115, WM-266–4, WM-793, C32, Sk-Mel-2, and Malme-3M) as well as from HaCaT keratinocytes and SV80 fibroblasts, loaded for comparison, were probed with antibodies against classical cads (N-, E-, and P-cad and cad 11), arm-type plaque proteins of adhering junctions (β-cat, protein $p120^{ctn}$, plakoglobin, and neurojungin), desmosomal cads (Dsg1–3 and Dsc1–3), and desmosomal plaque proteins (desmoplakin and PKP1–3). Five of the seven melanoma cell lines contain N-cad, two possess E-cad, four show P-cad and cad 11 is only found in one line. Interestingly, two melanoma lines, MeWo and C32, synthesize the desmosomal cad Dsg2, in the absence of all other desmosomal cads, a finding confirmed by immunoblotting with three different Dsg2 mAbs (clones DG3.10, 6D8, and 10G11). PKP1–3 are found in WM-115 cells and PKP3 occurs as the single PKP in MeWo cells, which, surprisingly, also contain the neuronal-type component of special kinds of adhering junctions (cf. Paffenholz *et al.*, 1999). *For immunoblot detection of Dsg1, whole cell lysates of human epidermis were loaded as positive control instead of HaCaT cell lysates.

Analyses of tight junction proteins revealed proteins ZO-1 and -2 in all melanoma cell lines examined (Table 1; see also Smalley *et al.*, 2005). However, proteins ZO-1 and -2 can occur both at adhering and at tight junctions (Itoh *et al.*, 1993, 1999) and indeed, it has been shown that in melanoma cells, ZO-1 is associated with adhering junctions (Smalley *et al.*, 2005). All other tight junction proteins probed, including the transmembrane constituents occludin and claudins 1 and 4, were not detected.

Clearly, the most unexpected result was the detection of Dsg2 in cells devoid of almost all other desmosomal constituents. To substantiate further this finding, PCR analysis was performed and the expected Dsg2 fragments were seen in both MeWo and C32 cells (Figure 3a). As another group had reported the detection of Dsg1 in different melanoma cell lines (Li *et al.*, 2001b), a finding contrasting with our own immunoblot results, we also conducted PCR experiments with Dsg1-specific primers. However, no amplification was seen in the melanoma lines (Figure 3a).

To identify candidates for interaction with Dsg2, lysates from lines C32 (Figure 3b) or MeWo (data not shown) were subjected to IP, followed by SDS-PAGE and matrix-assisted laser desorption ionization–time-of-flight analysis. In the Dsg2 immunoprecipitates, a ~160-kDa band appeared, which was identified as Dsg2 (Figure 3b, lane 3), but no other protein was specifically enriched. By contrast, in control IPs with β-cat antibodies, a 130-kDa band, corresponding to N-cad, and a 90 -kDa band representing α-cat were coimmunopreciptated with β-cat (Figure 3b, lane 4), that is, known functional protein complexes of adhering junctions. Essentially the same IP results were obtained in MeWo cells.

Subcellular localization of Dsg2 in melanoma lines

When we determined the subcellular distribution of Dsg2 by confocal microscopy, Dsg2 enrichment was observed at sites of cell–cell contacts, but also along free plasma membrane boundaries (Figure 4d and f). The classic plaque protein, β-cat, examined for comparison and control, was also accumulated at intercellular junctions, but appeared weaker at free cell borders (Figure 4b, c, e, and f) and did not codistribute with Dsg2 (Figure 4f). On the contrary, double labelling for β-cat and N-cad gave near-complete colocalization (Figure 4a–c) and the same applied for the comparison of α-cat and protein $p120^{ctn}$ (data not shown). When MeWo cells were labelled for PKP3 and neurojungin and C32 cells for plakoglobin, all three proteins were diffusely distributed, without any specific enrichment at a distinct structure, and this was observed with different fixation and staining protocols (data not shown; see Materials and Methods). Co-IPs in MeWo cells did not reveal interactions of Dsg2 with PKP3 or β-cat (Figure 4g). When C32 cell lysates were immunoprecipitated with Dsg2 antibodies, minor amounts of plakoglobin were pulled down and a weak plakoglobin band also appeared in β-cat immunoprecipitates (data not shown). Yet, similar as in MeWo cells, Dsg2 and β-cat did not coimmunoprecipitate. Moreover, like in WM35 cells, no co-IP of N- with P-cad was observed (data not shown).

Table 1. Detection of proteins associated with adhering junctions, desmosomes, and tight junctions in different melanoma cell culture lines

	MeWo	WM-115	WM-226-4	WM-793	C32	SK-Mel-2	Malme-3M	WM35
Adhering junction proteins								
N-cadherin	+	+	+	+	+	–	–	+
E-cadherin	–	–	–	–	–	+	+	+
P-cadherin	–	+	–	–	+	+	+	+
VE-cadherin	–	–	–	–	–	–	–	–
Cadherin 11	–	+	–	–	–	–	–	–
Cadherin 6	–	–	–	–	–	–	–	–
α-catenin	+	+	+	+	+	+	+	+
β-catenin	+	+	+	+	+	+	+	+
$p120^{ctn}$	+	+	+	+	+	+	+	+
Vinculin	+	+	+	+	+	+	+	+
α-Actinin	+	+	+	+	+	+	+	+
Plakoglobin[1]	(+)	(+)	+	+	+	+	+	+
ZO-1[2]	+	+	+	+	+	+	+	+
ZO-2[2]	+	+	+	+	+	+	+	+
Drebrin[3]	+	+	+	+	+	+	+	+
Neurojungin	+	–	–	–	–	–	–	–
Desmosomal proteins								
Desmoglein 1	–	–	–	–	–	–	–	–
Desmoglein 2	+	–	–	–	+	–	–	–
Desmoglein 3	–	–	–	–	–	–	–	–
Desmocollin 1	–	–	–	–	–	–	–	–
Desmocollin 2	–	–	–	–	–	–	–	–
Desmocollin 3	–	–	–	–	–	–	–	–
Plakophilin 1	–	+	–	–	–	–	–	–
Plakophilin 2	–	+	–	–	–	–	–	–
Plakophilin 3	+	+	–	+	–	–	–	–
Desmoplakin 1	–	–	–	–	–	–	–	–
Desmoplakin 2	–	–	–	–	–	–	–	–
Plakoglobin[1]	(+)	(+)	+	+	+	+	+	+
Tight junction proteins								
ZO-1[2]	+	+	+	+	+	+	+	+
ZO-2[2]	+	+	+	+	+	+	+	+
Occludin	–	–	–	–	–	–	–	–
Claudin 1	–	–	–	–	–	–	–	–
Claudin 4	–	–	–	–	–	–	–	–

[1]Plaque component of both adhering junctions and desmosomes.
[2]Proteins occurring both at adhering and at tight junctions.
[3]For references with respect to adhering junction localization, see Peitsch *et al.* (1999, 2005).
(+) Trace amounts detectable by immunoblot analysis.

To clarify the molecular complement of melanoma cell junctions and, in particular, the localization of Dsg2, we performed electron and immunoelectron microscopy of MeWo cells (Figure 5). Ultrathin sections revealed small plaque-bearing adhering junctions of the puncta adhaerentia category (Figure 5a–c; arrows) the plaques of which showed associations with actin microfilaments as well as lateral neighborhood to intermediate-sized filaments (Figure 5b and c). In molecular terms, these puncta junctions were identified by their cat and $p120^{ctn}$ components, and immunoelectron microscopy in general showed marked and specific enrichment in their plaques (Figure 5d–f; arrowheads). In addition, minor β-cat reactions could also be detected in junction-free plasma membrane regions (Figure 5d and e; arrows). Dsg2

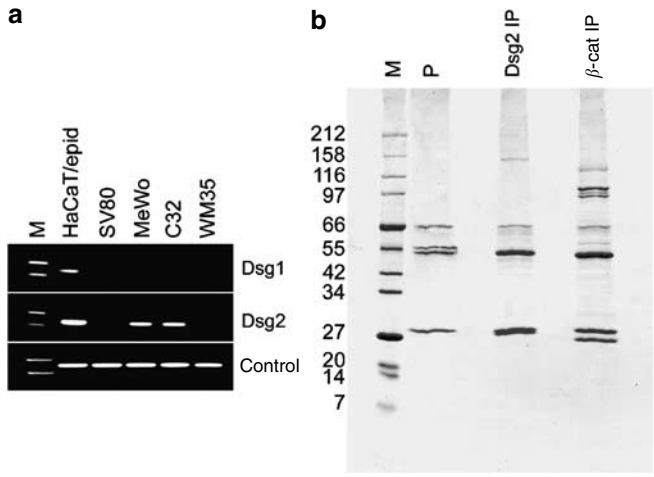

Figure 3. Specific detection of Dsg2 in MeWo and C32 cells at the mRNA level and by matrix-assisted laser desorption ionization–time of flight analysis. (**a**) PCR analysis of MeWo, C32, and WM35 melanoma cells using primers specific for the Dsg1 and 2 as well as for the actin-binding protein drebrin. Dsg2 is detected in MeWo and C32 melanoma cells, whereas none of the melanoma lines analyzed contains Dsg1. Human split skin has been employed as positive control for the Dsg1 PCR, HaCaT keratinocytes for the Dsg2 PCR, and SV80 cells as negative control. Size markers: 396 and 356 bp (Dsg1 and Dsg2 PCR) or 356 and 247 bp (drebrin PCR). (**b**) Coomassie blue-stained 4–20% acrylamide gel, showing proteins immunopreciptated from C32 cell lysates with antibodies to Dsg2 or β-cat. In the Dsg2 immunoprecipitate, a solitary band of ~160 kDa is seen, which has been identified as Dsg2 by matrix-assisted laser desorption ionization–time of flight analysis. In the β-cat immunoprecipitate, a band at ~130 kDa represents N-cad, and bands at 90–100 kDa contain α- and β-cat. Further bands at 66, 55, and ~30 kDa correspond to bovine serum albumin and the heavy and light Ig chains of the antibodies. P, material of the preclearing step; M, molecular weight marker, as indicated on the left margin.

was seen along the entire cell surface, but without any specific enhancements at plaques (Figure 5g).

Distribution of adhering junction proteins and Dsg2 in coculture systems

To assess the possible role of Dsg2 and the adhering junction proteins in heterotypic cell–cell adhesions of melanoma cells, coculture systems confronting melanoma cells with fibroblasts or keratinocytes of line HaCaT were established. When two-dimensional MeWo cell-fibroblast cocultures were reacted with antibodies to adhering junction proteins, including N-cad, α- and β-cat, and protein p120^{ctn}, they all labelled homotypic fibroblast and homotypic melanoma junctions as well as heterotypic melanoma–fibroblast junctions. As an example, the reaction of N-cad is shown in Figure 6a. Dsg2 staining of such cocultures revealed absence of this protein from fibroblasts, as expected, but demonstrated enrichment at the homotypic cell borders of MeWo cells (Figure 6c). In cocultures of C32 (Figure 6e–j) or MeWo cells with HaCaT keratinocytes, E-cad and desmosomal cads, except Dsg2, appeared exclusively in the keratinocytes: E-cad in linear arrays representing the series of adhering junctions (Figure 6e and f), the desmosomal proteins in their typical punctate arrays (data not shown). In contrast, reaction sites of β-cat (Figure 6g and h) as well as of α-cat, and protein p120^{ctn} (data not shown) were accumulated both along homotypic adhering junctions of melanoma and HaCaT cells and in regions indicative of heterotypic contacts. Correspondingly, Dsg2 was seen at the heterotypic interaction borders between melanoma and HaCaT cells (Figure 6i and j).

As a cell culture model of the situation *in vivo* organotypic cultures of MeWo or C32 cells with HaCaT keratinocytes were prepared. Keratinocytes and melanoma cells were mixed in a 5:1 ratio, corresponding to the physiological ratio in the basal epidermal layer and these cultures were exposed to an air–liquid interface for two weeks to allow differentiation of the keratinocytes and formation of a stratified epidermal equivalent (Figure 7). In MeWo–HaCaT organotypic cocultures, MeWo cells, a line originally generated from a melanoma lypmph node metastasis (cf. Table 3), formed cell clusters in subepidermal nests (Figure 7a–f). Immunostainings for β-cat (Figure 7a and b) and other adhering junction plaque proteins (data not shown) were positive not only at homotypic junctions between the keratinocytes on the one hand and MeWo cells on the other, but also at contact sites between the basal keratinocytes and the subepidermally located melanoma cells (Figure 7b). Dsg2 was detected in remarkable intensity at the MeWo cell contacts as well as in the basal layer of the epidermal equivalent, corresponding to the situation *in vivo* and at the boundaries between MeWo cells and basal keratinocytes (Figure 7e and f). By contrast, the reactions for Dsg 1 were rather inverse, showing strongly positive reactions in the upper epidermal layers. Clearly, this protein was absent from the melanoma cells (Figure 7c and d; cf. Figure 7i and j). Different from the MeWo cells, cells of the line C32 originated from a primary amelanotic melanoma, did not invade the epidermal equivalent but formed a compact multilayer tumor on top of it (Figure 7g–l). Otherwise, the distribution pattern of the adhering junction-associated and desmosomal proteins was similar to that noted in the MeWo–HaCaT organotypic cocultures.

Cad patterns in melanoma metastases *in situ*

To verify whether our results with cell culture systems might also be relevant for genuine tumors *in situ*, small samples of melanoma metastases from 10 different patients, originating from skin, lymph node, or lung tissue, all positive for melan-A, were analyzed by immunofluorescence microscopy (Figure 8 and Table 2). Eight of 10 metastases contained N-cad, enriched along cell boundaries (Figure 8a, c, d, f, j, and l) and in seven of the 10 metastases, at least a subpopulation of the tumor cells was positive for E-cad (cf. Figure 8e, f, n, and o and Table 2). Coexistence of both classical cads was noted in six metastases and double-label confocal microscopy revealed that they could occur both separately in different cell clusters and together within the same cell (Figure 8f). P- and VE-cad were detected each in two of 10 metastases, but only in small cell groups, representing less than 20% of the tumor cells (Table 2). Interestingly, two metastases contained some cells positive

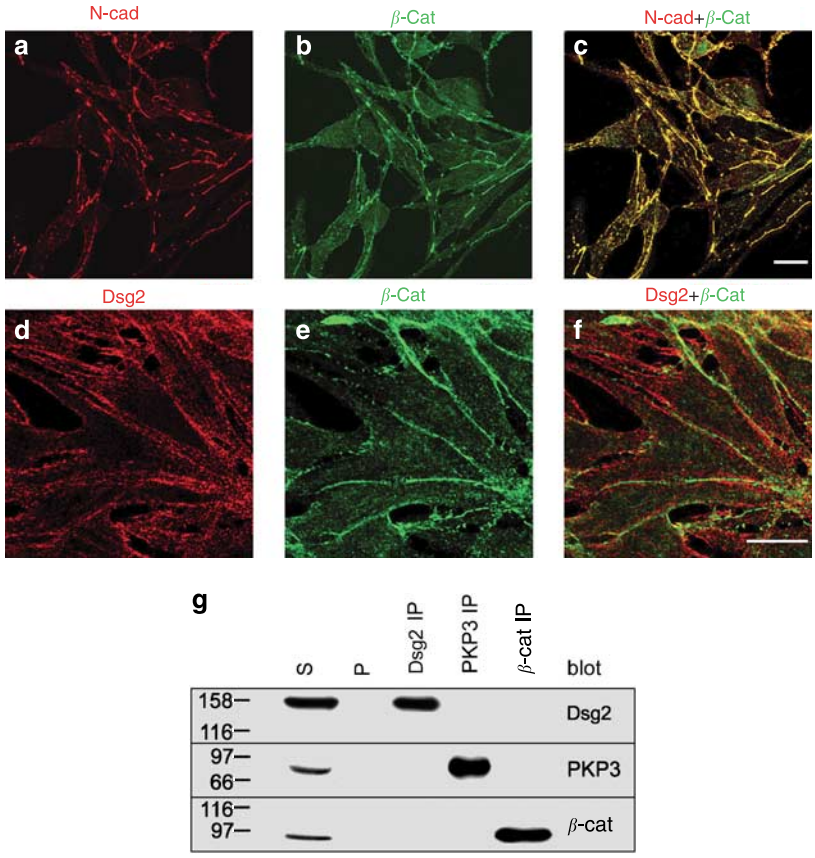

Figure 4. Differential distribution of Dsg2, compared with adhering junction proteins, in cultured melanoma cells. (**a**–**f**) Confocal microscopy of MeWo melanoma cells, stained for β-cat (green in **b**, **c**, **e**, and **f**) in combination with N-cad (red in **a** and **c**) or with Dsg2 (red in **d** and **f**). All three proteins are enriched at intercellular junctions and along free cell boundaries. Although β-cat and N-cad show (**c**) far-reaching colocalization , (**f**) localizations of β-cat and Dsg2 are completely distinct. Bar = 20 μm. (**g**) IP and immunoblot analysis of MeWo cell lysates with antibodies to Dsg2, PKP3, and β-cat, showing no co-IP, indicating that in the specific lysate they occur in different protein complexes.

for Dsg1, which at least, in one of these, appeared enhanced at cell boundaries (Table 2). Moreover, and most remarkably, Dsg2 was found in five of the 10 metastases and in four of them, even more than 50% of the tumor cells were positive (Table 2 and Figure 8g–o). As to subcellular distribution, significant cell border enrichment was noted in three of the five Dsg2-positive metastases (cf. Figure 8g, i, j, m, l, o), whereas the other two showed diffuse cytoplasmic staining (data not shown). When the Dsg2-positive metastases were double-labelled with antibodies to N- (Figure 8j–l) or E-cad (Figure 8m–o), it was evident that Dsg2 could occur both in N- and E-cad-containing cells (Figure 8l and o), apparently independent of the two classical cad pattern.

Surprisingly, in one metastasis, no. 864, which in its histology did not markedly differ from the other metastases, neither N-, E-, VE-, nor P-cad and cad 11 immunostaining was significant along cell–cell boundaries. However, most cell borders were labelled by antibodies against α- and β-cat and protein $p120^{ctn}$. Moreover, a variable number of tumor cells were positive for Dsg1, 2, and 3, all appearing accumulated along cell boundaries, whereas desmosome-specific plaque proteins were not detected by immunofluorescence microscopy. Therefore, we decided to extend our research on this specific subtype to a greater number of tumors.

Together, our observations *in situ* indicated that the cad patterns and combinations were more variable than anticipated and that metastases could comprise extremely heterogeneous subcompartments, reflecting our observations *in vitro*.

DISCUSSION

Our study has given three important results: first, the cad pattern of melanomas can be quite heterogeneous and certain melanoma cell lines as well as metastases can synthesize several – up to three – classical cads within the same cell. Second, a proportion of cultured melanoma cells and melanoma metastases contain, in addition, the desmosomal cad Dsg2, which, in the absence of desmosomes, is dispersed over the cell surface. Third, this complex cad complement contributes to the remarkable diversity of options of melanoma cells to form heterotypic cell–cell interactions. Thus, the facultative cad repertoire of melanoma cells might be much larger than previously thought, probably depending not only on the degree of malignancy but also on the specific growth conditions and the microenvironment.

Heterogeneous cad profiles and their implications

It is well known that under certain circumstances, melanoma cells can synthesize other cads than N- or E-cad. For example, P-cad has been identified in melanoma cells (Hsu *et al.*, 1996; Bauer *et al.*, 2005, 2006) and has been reported, similar to E-cad, to promote cell–cell adhesion and counteract invasion (Van Marck *et al.*, 2005). Moreover, the amount of P-cad appears to have a prognostic relevance, as a loss of P-cad is commonly seen in advanced melanomas and melanoma metastases (Bauer *et al.*, 2006). This seems in accordance with our findings on melanoma metastases in which only a very small subpopulation of cells was P-cad-positive. In addition to P-cad, melanoma cells may facultatively also synthesize VE-cad, a cad characteristic for endothelial cells, that has been related to highly aggressive melanoma cell lines undergoing ''vasculogenic mimicry'', a process facilitating hematogeneous metastasis (Hendrix *et al.*, 2001; Hess *et al.*, 2006). Our melanoma lines were all VE-cad-negative, but two of 10 metastases comprised small subgroups of VE-cad-positive cells.

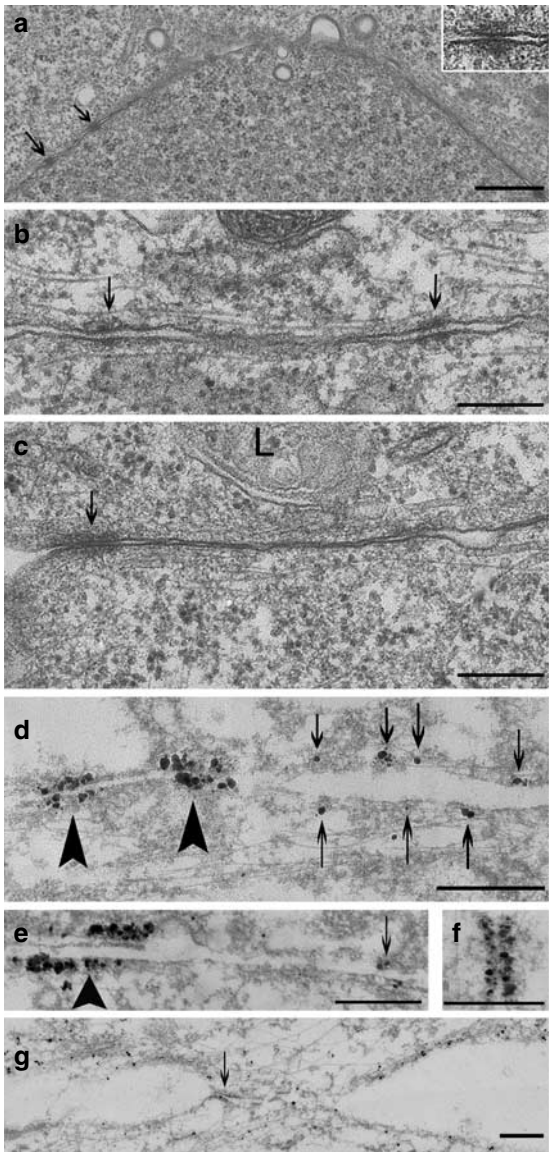

Figure 5. Electron and immunoelectron microscopy presenting cell–cell contacts of MeWo cells. (**a**–**c**) Conventional electron microscopy. In (**a**) the survey as well as in (**b** and **c**) more detailed, high-resolution micrographs, several small, plaque-bearing puncta adhaerentia junctions are seen (arrows in **a**–**c**; inset in **a**: higher magnification of such a junction). Note that at some sites devoid of plaques, the plasma membranes of neighboring cells are extremely close spaced, indicative of another form of junction (**c**). L, lysosome. Bar = 700 nm. (**d**–**g**) Immunoelectron microscopy, using (**d**–**f**) mAbs to β-cat and (**g**) to Dsg2 in combination with gold-coupled secondary antibodies and signal enhancement by the silver technique. β-cat is densely accumulated in the plaques of the puncta adhaerentia (arrowheads in **d** and **e**; higher magnification in **f**). Moreover, plaque protein reactions are sometimes also detected at plaque material of free plasma membranes (arrows in **d** and **e**). Dsg2 staining is observed diffusely along the plasma membrane, both at intercellular contact regions and along free cell membranes, with occasional weak reactions at plaques (arrow) but, in contrast to β-cat, does not show specific enrichment at these sites (**g**). Bar = 700 nm.

Surprisingly, one of eight melanoma cell culture lines examined in our study contained cad 11, a type II classical cad originally identified in osteoblasts but later also detected in diverse other cells of mesenchymal origin which had so far not been described in melanoma cells. In an earlier study, six novel, yet not further characterized cad fragments, termed ME1–ME6, have been identified in melanoma cell lines by PCR (Matsuyoshi *et al.*, 1997).

Heterogeneity of subpopulations of melanoma cells might also have important implications for the growth and spreading of these tumors *in situ*. Although E-cad is known to inhibit and N-cad to enhance proliferation, migration, and metastasis, different immunohistochemical investigations have shown that a proportion of melanoma metastases still contains significant E-cad amounts (Danen *et al.*, 1996; Silye *et al.*, 1998; Sanders *et al.*, 1999; Andersen *et al.*, 2004). In our study, one of 10 metastases contained E-cad as the only classical cad and six of 10 synthesized both E- and N-cad, occasionally in different subcompartments of the tumor but sometimes even within the same cell. Therefore, loss of E-cad is apparently not a universal or an inevitable feature of tumor metastasis. Alternatively, it could also be possible that in some melanomas, E-cad is only temporarily downregulated during tumor development, but re-expressed later in metastases. Remarkably, and in contrast to other melanoma subtypes, it has been reported for uveal melanoma that E-cad-containing tumors show an increased risk for metastasis (Onken *et al.*, 2006).

Our biochemical analyses in a melanoma cell line containing E-, N-, and P-cad together, have shown that all three cads form complexes with the same set of plaque proteins of adhering junctions, that is, α- and β-cat, plakoglobin, and protein $p120^{ctn}$. Yet, although E- and N- as well as P- and N-cad occur in different complexes, E- and P-cad have been found to coimmunoprecipitate. Traditionally, the cell–cell binding specificities of cads have been considered as primarily homotypic. However, more recent studies have shown that their interactions can also be more promiscuous (e.g., Shimoyama *et al.*, 2000; Niessen and Gumbiner, 2002; see the review Patel *et al.*, 2003). Results of studies in cocultures of lens and liver cells (Volk *et al.*, 1987) or of epithelial cells and fibroblasts (Omelchenko *et al.*, 2001) have been taken as indications of heterotypic

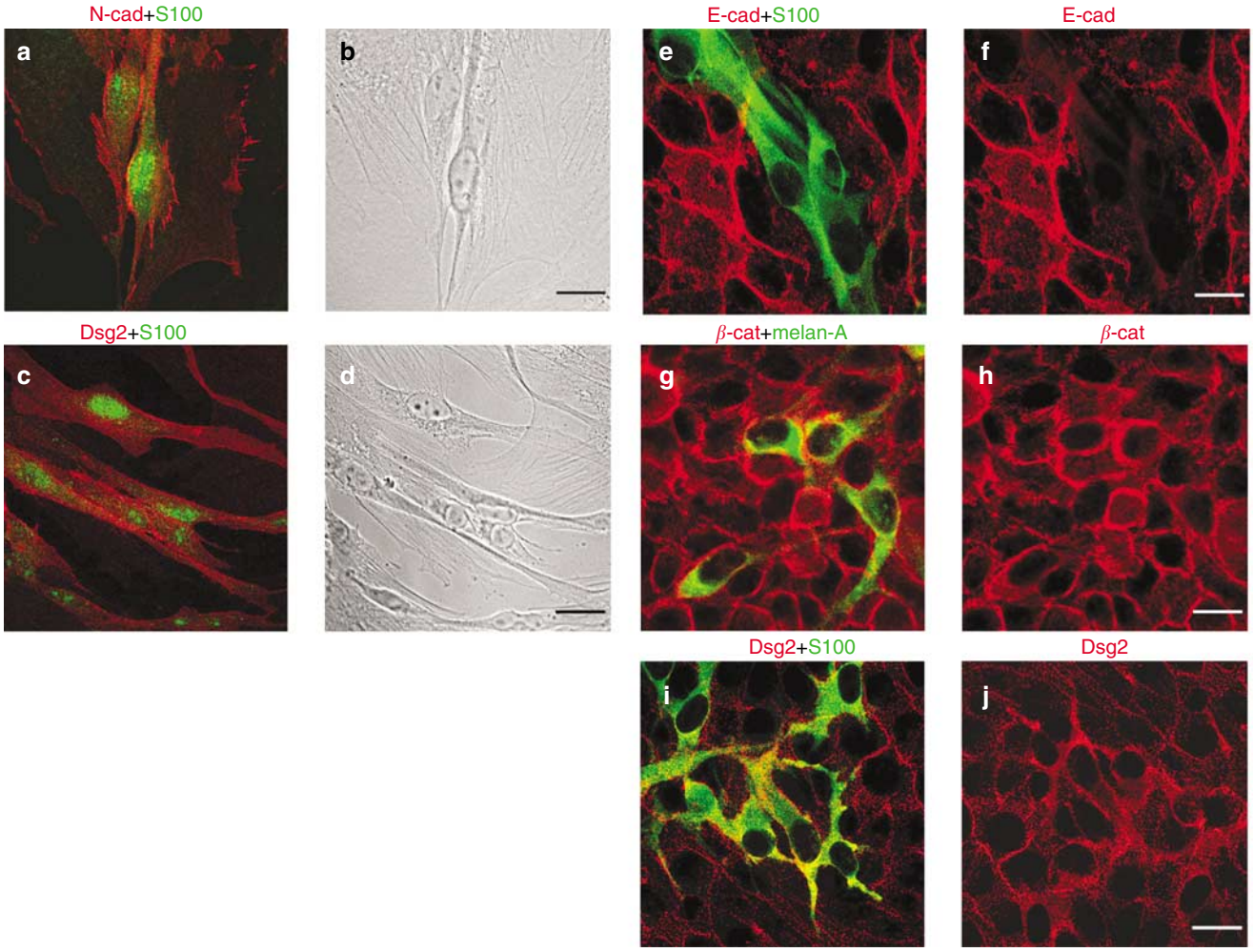

Figure 6. Localization of adhering junction proteins and Dsg2 in adherent cell cocultures. (**a**–**d**) Confocal microscopy of cocultures of primary human fibroblasts and MeWo melanoma cells, labelled for N-cad (red in **a**) or Dsg2 (red in **c**) in combination with S100 protein as melanoma marker (**a** and **c**; green). (**a**) N-cad is detected both in homotypic melanoma–melanoma and fibroblast–fibroblast junctions and in regions of heterotypic contacts between the two cell types, whereas Dsg2 staining is only seen on the surfaces of the S100-positive melanoma cells, here at intercellular contacts as well as along free cell membranes (**b** and **d**, phase contrast images). Bar = 20 μm. (**e**–**j**) Cocultures of HaCaT keratinocytes and C32 melanoma cells, immunostained for (**e** and **f**; red) E-cad, (**g** and **h**; red) β-cat, (**i** and **j**; red) Dsg2, and the melanoma cell markers, (**e** and **i**; green) S100 and (green in **g**) melan-A. (**e** and **f**) Here, E-cad is exclusively found along keratinocyte cell–cell borders containing adhering junctions. (**g** and **h**) By contrast, homotypic melanoma, homotypic keratinocyte, and heterotypic melanoma–keratinocyte contact sites are strongly positive for β-cat. (**i** and **j**) The same holds for Dsg2, which in HaCaT cells appears in the punctate pattern typical of demosomes. Bar = 20 μm.

adhesions formed by N- and E-cad. Moreover, L-cells transfected with E- or P-cad are capable of forming ''E–P heterocadherin'' adhesions between adjacent cells (Duguay *et al.*, 2003; Foty and Steinberg, 2005). On the other hand, it is now clear that certain cads may form lateral *cis*-heterodimers (e.g., Shan *et al.*, 2000) and specifically E- and P-cad *cis*-heterodimers have been identified in A431 carcinoma cells (Klingelhöfer *et al.*, 2000). As to the heterotypic E-P-cad complexes found in our study, their *cis*- or *trans*-nature remains to be determined.

Dsg2 as a novel solitary cell surface component characteristic of a subset of melanoma cells

A totally unexpected result of our study is that certain kinds of melanoma cells synthesize the desmosomal cad Dsg2, known as a widespread transmembrane glycoprotein of desmosomes of all proliferative epithelial cells, keratinocytes included (Schäfer *et al.*, 1994). Via its intracellular domain, Dsg2 interacts with plakoglobin which, in turn, can bind other desmosomal plaque proteins, the PKPs and desmoplakin, the latter constituting a linker to intermediate filaments (Troyanovsky *et al.*, 1993; Chitaev *et al.*, 1996; see the review Getsios *et al.*, 2004). In addition, Dsg2 is also an important constituent of the *area composita* complex connecting cardiomyocytes (Borrmann *et al.*, 2006; Franke *et al.*, 2006).

In our two melanoma cell lines, the Dsg2 distribution was radically different from that known from all other cell types. Here, the adhesive glycoprotein was spread over the cell surface, with occasional clusters at otherwise inconspicuous cell–cell contact sites. Biochemically, it was not found in

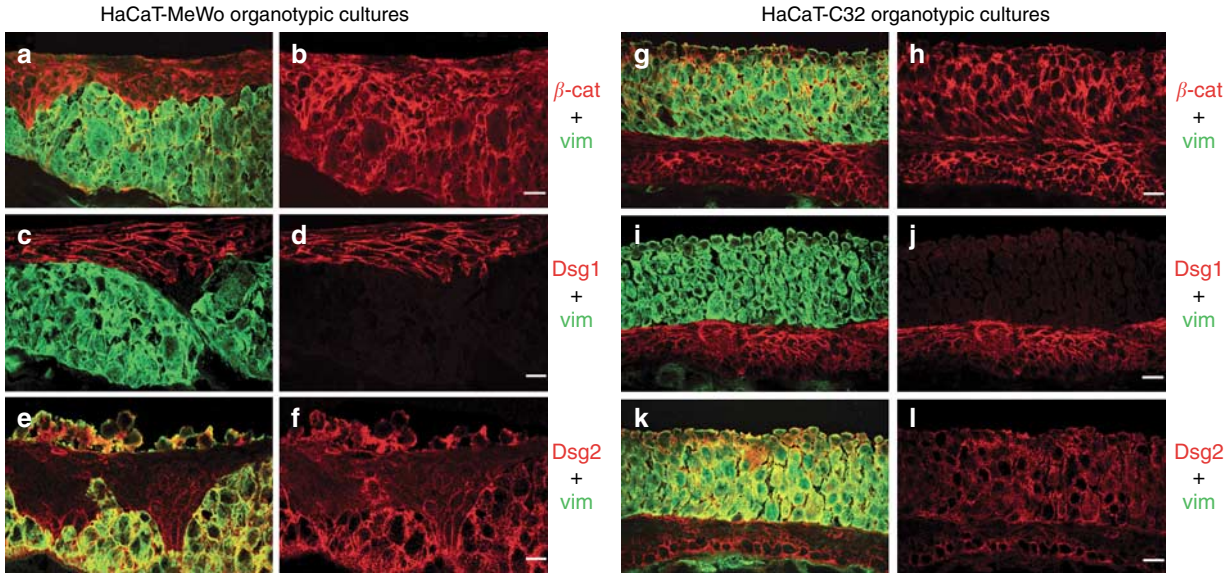

Figure 7. Immunolocalizations of junctional proteins in organotypic keratinocyte-melanoma cell cocultures. Vimentin (green in **a–k**) has been generally used as marker protein for the identification of melanoma cells. (**a–f**) In organotypic cultures of HaCaT keratinocytes with melanoma cells of line MeWo, the keratinocytes form a stratified and differentiated epidermis with a stratum corneum equivalent layer on top, whereas cells of line MeWo, derived from a lymph node metastasis, are densely aggregated in subepidermal cell clusters. As seen by double-label confocal microscopy, β-cat antibodies (**a** and **b**; red) mark homotypic junctions, both between keratinocytes and between melanoma cells as well as regions of heterotypic contacts between the HaCaT and the MeWo cells. Dsg1-positive reactions (**c** and **d**; red) are exclusively observed in the epidermis and here mostly in the upper layers. Clearly, the MeWo cells appear Dsg1-negative. By contrast, Dsg2 (**e** and **f**; red) is enriched in the basal epidermal layer. Moreover, strong Dsg2 immunoreactions are noted at junctions between the subepidermal MeWo cells as well as in areas of heterotypic MeWo cell–keratinocyte contacts. Bar = 20 μm. (**g–l**) In organotypic cocultures confronting HaCaT keratinocytes with C32 cells, originated from a primary melanoma, the melanoma cells do not invade the epidermal equivalent but form a dense multilayer conglomerate on top of it. Double-label confocal microscopy, using (**g** and **h**; red) antibodies to β-cat, (**i** and **j**; red) Dsg1, and (**k** and **l**; red) Dsg2, in combination with (**g–k**; green) vimentin as a melanoma cell marker, reveals distribution patterns for β-cat and the desmosomal cads Dsg1 and 2 that are similar to those in the organotypic HaCaT-MeWo cell cocultures. Bar = 20 μm.

complexes with any other junctional proteins. A similar cell surface distribution of Dsg2 was observed in the human fibrosarcoma cell line HT-1080, the only cell line reported so far to contain endogenous Dsg2 but no other desmosomal constituents (Chitaev and Troyanovsky, 1997). When this cell line was stepwise transfected with other desmosomal cads, junction protein complexes were formed. It was even possible to induce the formation of desmosomes by cotransfection of the other desmosomal proteins, of which the plaque protein, PKP2, played an especially important anchoring role (Koeser *et al.*, 2003).

When we systematically examined our Dsg2-positive melanoma cell lines for other desmosomal proteins, we only found plakoglobin, a constituent of both desmosomes and adhering junctions, which was synthesized in C32 cells in minor amounts and only in traces in MeWo cells. In addition, in MeWo but not in C32 cells, PKP3 was detected, another member of the $p120^{ctn}$ family of armadillo-related proteins (see the review Schmidt and Jäger, 2005). However, as seen by immunolocalization, both plakoglobin and PKP3 occurred predominantly in the cytoplasm and only small amounts of plakoglobin coimmunoprecipitated with Dsg2 in C32 cells. Thus, so far, Dsg2 appears as a primarily solitary cell surface component. This raises the question whether it can in fact as a single molecule type exert significant adhesive strength. When L-cells, a mouse fibroblast line, were transfected with cDNAs encoding single desmosomal cads or related chimeric proteins in the absence of other desmosomal components, the adhesive properties of the transfectants were only very weak (Amagai *et al.*, 1994; Chidgey *et al.*, 1996; Kowalczyk *et al.*, 1996). However, in contrast to our melanoma cell lines, these transfected L-cells were said to be devoid of any functional adhering junctions and thus may lack initiating components for desmosome formation (see the review Getsios *et al.*, 2004).

Another group has reported the synthesis of Dsg1 in several melanoma cell lines and its downregulation by autocrine hepatocyte growth factor, in parallel with down-regulation of E-cad (Li *et al.*, 2001b). In all the melanoma cell lines we analyzed, including line WM35 used by Li *et al.* (2001b), we did not detect Dsg1, neither at protein nor at the mRNA level. On the other hand, our observation that the Dsg1 antibody also used by Li *et al.* (clone 62, from BD Biosciences Pharmingen; Heidelberg, Germany), not only reacted with a 160-kDa band present in all melanoma cell lines but also in fibroblasts used as negative control as well as our matrix-assisted laser desorption ionization results that the 160-kDa component immunoprecipicated with this antibody was identified as epidermal growth factor receptor (data not shown) led us to the conclusion that this represents, most probably, a cross-reaction of this antibody between the two proteins.

Table 2. Classical and desmosomal cadherins in melanoma metastases in the lung, LN, or skin

Case no.	MM 770	MM 761	MM 782	MM 841	MM 864	MM 906	MM 941	MM 944	MM 948	MM 962
Primary melanoma	MUP	SSM, back, 1.03 mm, Clark level III	NM, shoulder, 1.5 mm, Clark level IV	NM, back, 4.5 mm	NM, chest, 1.0 mm, Clark level IV	SSM, chest, 1.9 mm, Clark level IV	Type unknown, shoulder, 3 mm	NM, knee, 4.0 mm, Clark level IV	NM, upper arm, 4.0 mm, Clark level III	Pedunculated, ulcerated melanoma shoulder, 2.6 mm
Metastatic site	Lung	LN, supraclavicular	LN, groin	LN, axilla	Lung	Skin, axilla	LN, groin	LN, groin	Skin, shoulder	Skin, abdomen
Cadherin pattern in metastases										
Classical cads										
N-cad	+	+++	+++	++	–	+++	–	+++	+++	+++
E-cad	+++	–	++	+	–	–	++	+++	+++	+++
P-cad	–	–	–	–	–	–	+	–	–	+
VE-cad	+	–	+	–	–	–	–	–	–	–
Desmosomal cads										
Dsg1	+	–	–	–	+++	–	–	–	–	–
Dsg2	+	+++	++	–	++	–	–	–	–	+++

LN, lymph node; MUP, melanoma of unknown primary; NM, nodular melanoma; SSM, superficial spreading melanoma.
Metastases with ⩾10% but <50% immunoreactive tumor cells were classified as ''+'', those with 50–75% reactive cells as ''++'', and those with ⩾75% as ''+++''.

We have identified Dsg2 not only in monocultures of melanoma cells but also in two- or three-dimensional cocultures and in regions of both homotypic melanoma cell and heterotypic melanoma–keratinocyte contacts. This implies the possibility that Dsg2 can indeed act as a heterotypic cell–cell adhesion molecule between keratinocytes and melanoma cells. It will therefore be mandatory to investigate the ultrastructural basis of such heterotypic contacts, especially as keratinocytes contain desmosomes and melanoma cells do not. Moreover, it will be important to characterize the subgroup of Dsg2-positive melanoma cells in greater detail and its impact on melanoma progression and metastasis. In this context, it may be remarkable that in our organotypic cocultures, one of the Dsg2-positive lines, C32, originated from a primary amelanotic melanoma, did not invade into the artificial epidermis, whereas the other line, MeWo, derived from a lymph node metastasis, formed subepidermal melanoma cell nests as well as Dsg2-positive contact sites with the basal keratinocytes.

Furthermore, it will be interesting to investigate normal melanocytes for Dsg2. Indeed, our studies on normal human epidermal melanocytes, both from newborn foreskin (NHEM-f_1, PromoCell, Heidelberg, Germany) and from adult skin (NHEM-a_1, PromoCell), cultured in serum-free medium, have shown some amounts of Dsg2, both on RNA and on protein level (unpublished results).

Together, our data indicate that a non-desmosome-integrated, ''free'' cell surface glycoprotein Dsg2 might represent a novel, primitive cell–cell adhesion system characteristic of a certain subset of melanomas. We propose to differentiate this subtype of melanoma cells in pathological diagnosis and to characterize it in detail with respect to interaction partners and regulatory proteins involved as well as with respect to its adhesive strength and pathophysiological implications, notably the tumor behavior of the Dsg2-positive melanomas.

MATERIALS AND METHODS

Antibodies

Murine mAbs against N-, E-, and P-cad (clone 56), Dsg1 (clone 62), α- and β-cat, and protein $p120^{ctn}$ were purchased from BD Biosciences Pharmingen, whereas mAbs against vinculin (clone 11–5) and α-actinin (clone BM-75.2) as well as rabbit antisera to α- or β-cat were obtained from Sigma (Deisenhofen, Germany). A rabbit antiserum to N-cad was from QED Bioscience Inc. (San Diego, CA) and a rabbit mAb to E-cad from Epitomics (obtained through Biomol GmbH, Hamburg, Germany). Other mAbs, directed against cad 11, P-cad (clone NCC-CAD-299), Dsg1 and 2 (clones 27B2 and 6D8), and claudin 4 were obtained from Invitrogen (Karlsruhe, Germany), as were polyclonal rabbit antibodies against proteins ZO-1 and -2, occludin, and claudin 1. A cad 6 mAb was from USBiological (obtained through Acris, Hiddenhausen, Germany) and a pan-Dsc rabbit antiserum (clone AHP 322) from Serotec (Düsseldorf, Germany). A mAb directed against cad 5 (VE-cad; clone BV9) was kindly provided by Professor Elisabetta Dejana (Department of Biomolecular and Biotechnological Sciences, School of Sciences, University of Milan, Italy; cf. Lampugnani *et al.*, 1992). The neurojungin mAb was from Dr Rainer Paffenholz (Ingenium

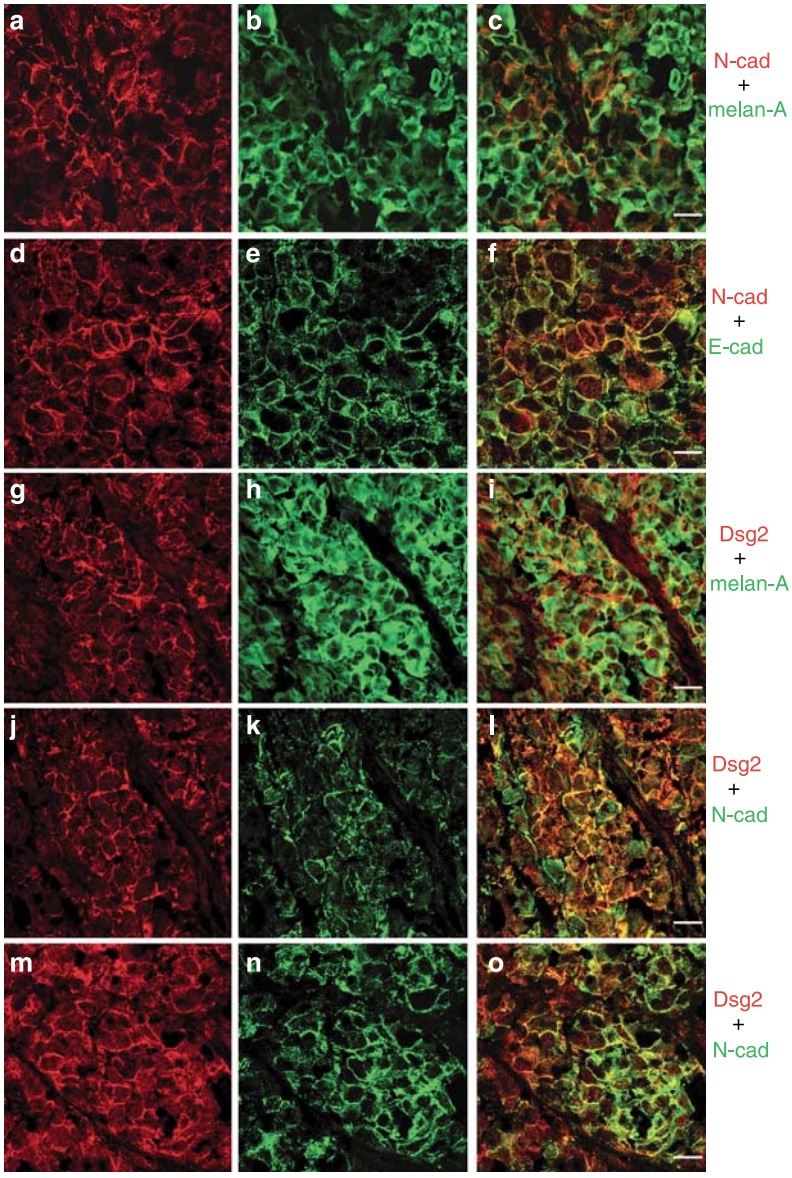

Figure 8. Double-label confocal microscopy presenting heterogeneous cad patterns in melanoma metastases. Cryostat sections of metastasis no. 962 (exemplatory shown) have been labelled with antibodies to N-cad (Red in **a**, **c**, **d**, and **f**; green in **k** and **l**), E-cad (**e**, **f**, **n**, and **o**; green), and Dsg2 (red in **d**–**m** and **h**–**o**) as well as with the melanoma cell marker melan-A (**b**, **c**, **h**, and **i**; green). In the metastasis presented, the vast majority of the melanoma cells exhibit strongly positive N-cad staining at cell–cell junctions (**a** and **c**; red). A major subset of the tumor cells also contains (**e** and **f**, green) E-cad, often appearing in the same cells as (**f**) N-cad. Moreover, large cell clusters also synthesize the desmosomal cad (**g**, **j**, **m**; **i**, **l**, **o**, red) Dsg2, which is markedly enriched along the cell borders. This protein can occur in melanoma cells containing (**l**) N-cad as well as in those positive (**o**) for E-cad, thus appearing independent of the classical cad profile. Bar = 20 μm.

Pharmaceuticals AG, Martinsried, Germany; cf. Paffenholz *et al.*, 1999) and for the demonstration of plakoglobin, a mAb (clone 11E4) from Professor Margaret J. Wheelock (University of Nebraska Medical Center, Omaha, NE) was used. Rabbit antibodies against Dsg2 (clone rb5) were a gift from Dr Lutz Langbein, guinea-pig antibodies against vimentin (clone GP1) from PD Dr. Ilse Hofmann (both Division of Cell Biology, German Cancer Research Center, Heidelberg, Germany). The following antibodies against desmosomal and other cytoskeletal proteins, most of which were generated in the Division of Cell Biology of the German Cancer Research Center, were purchased from Progen Biotechnik (Heidelberg, Germany): mAbs against desmoplakins 1 and 2 (clones DP-2.15, -2.17, and -2.20; Moll *et al.*, 1986), plakoglobin (clone PG 5.1; Cowin *et al.*, 1986), PKP1, 2, and 3 (clones PP1–2D6, PP2/86, and PKP3–270.6.2, respectively; Heid *et al.*, 1994; Mertens *et al.*, 1996; Schmidt *et al.*, 1999), Dsc1 and 3 (clones Dsc1-U100 and Dcs3-U114; Nuber *et al.*, 1996); Dsg1 (clone Dsg1-P23; Kurzen *et al.*, 1998), Dsg1 and 2 (clone DG 3.10; Schmelz *et al.*, 1986), Dsg2 (clone 10G11; Schäfer *et al.*, 1994), Dsg3 (clone Dsg-G194; Kurzen *et al.*, 1998), vimentin (clone VIM 3B4), and drebrin (clone MX823; Peitsch *et al.*, 2005). As melanoma markers, a mAb against melan-A and a rabbit antiserum against S100 protein (both from Progen Biotechnik) were used.

Table 3. Origins of the different melanoma cell culture lines used in this study

Melanoma cell line	Origin
MeWo	Lymph node metastasis
WM-115	Primary melanoma, skin
WM-266-4	Skin metastasis
WM-793	Primary melanoma, skin (SSM, vertical growth phase)
C32	Primary melanoma, skin (amelanotic melanoma)
SK-Mel-2	Skin metastasis
Malme-3M	Lung metastasis
WM35	Primary melanoma, skin (SSM, vertical and radial growth phase)

SSM, superficial spreading melanoma.
All lines were obtained from American Type Culture Collection.

For immunofluorescence microscopy, primary antibody complexes were visualized with secondary antibodies coupled to Cy3 (Dianova, Hamburg, Germany) or Alexa 488 (MoBiTec, Göttingen, Germany). For immunoblot analysis, horseradish peroxidase-conjugated secondary antibodies were applied in combination with the enhanced chemiluminescence system (NEN, Köln, Germany).

Cell culture

Human melanoma cells of lines MeWo, WM-115, WM-266–4, WM-793, C32, SK-Mel-2, Malme-3M, and WM35 as well as Simian virus (SV40)-transformed human SV80 fibroblasts and human U333 glioma cells were provided by American Type Culture Collection (Manassas, VA; for origins of the different melanoma lines, see Table 3). HaCaT keratinocytes were obtained from Professor Petra Boukamp (Genetics of Skin Carcinogenesis, German Cancer Research Center; Boukamp *et al.*, 1988). All cell lines, except WM35, were cultured in DMEM (Invitrogen) supplemented with 10% fetal calf serum (FCS; Biochrom, Berlin, Germany) and 2 mM glutamine. WM35 cells were propagated in a 4:1 mixture of MCDB 153 medium (with 1.5 g/l sodium bicarbonate) and Leibovitz's L-15 medium (both from Biochrom), supplemented with 2 mM L-glutamine, 0.005 mg/ml bovine insulin, 1.68 mM $CaCl_2$, and 2% FCS. For isolation of primary human fibroblasts, human dermis was washed with phosphate-buffered saline (PBS) and cut into small pieces, which then were placed on glass coverslips and transferred into culture flasks containing DMEM plus 10% FCS, 2 mM glutamine, and 100 U/ml penicillin/streptomycin (Invitrogen). Cells were subcultured for the first time after ~2 weeks and were used for experiments in passage 4. Preparation and cell culture of human umbilical vein endothelial cells, used as controls for VE-cad immunoblots, was as reported previously (Peitsch *et al.*, 1999). All cell lines were maintained at 37°C with 5% CO_2 and subdivided twice a week.

For two-dimensional melanoma–fibroblast or melanoma–keratinocyte cocultures, cells were trypsinized, counted in a Neubauer chamber, and seeded on glass coverslips in a 5:1 ratio (fibroblasts: melanoma cells or HaCaT:melanoma cells, respectively). Cocultures were maintained for 3–4 days in DMEM plus 10% FCS before procession for immunofluorescence analysis.

Organotypic cocultures

Organotypic cocultures were prepared essentially as described by Stark *et al.* (1999). Dermal equivalents were generated with native type I collagen extracted from rat-tail tendons. The lyophilized collagen was redissolved with 0.1% acetic acid (final concentration: 4 mg/ml) and eight volumes of ice-cold collagen solution were mixed with one volume of 10 × Hank's buffered saline, followed by neutralization with NaOH up to a pH value of 7.0. Fibroblasts were trypsinized, counted, and resuspended in 100% FCS. One volume of fibroblast/FCS solution was added, resulting in a final concentration of 3.2 mg/ml collagen and 2×10^5 cells/ml. Of this mixture, 2.5 ml each were poured into PET membrane filter inserts (Falcon no. 3090, BD Biosciences), placed into special deep six-well trays (Biocoat 355464, BD Biosciences) and allowed to harden for 1 hour at 37°C. Glass rings (24 mm outer, 20 mm inner diameter) were put on the gels to compress them and to provide a central flat area for keratinocyte seeding. The gels were equilibrated over night with DMEM supplemented with 10% FCS and with 50 μg/ml ascorbic acid (Sigma). In total, 1×10^6 cells were seeded. The next day, HaCaT keratinocytes (passage 40), mixed with MeWo or C32 melanoma cells in a 5:1 ratio, were seeded on the top of the collagen matrix using DMEM with 10% FCS and 50 μg/ml ascorbic acid as culture medium, supplemented, for the first week, with 2 ng/ml epidermal growth factor (PromoCell) and 2 ng/ml transforming growth factor-α (R&D Systems, Minneapolis, MN). After submerse incubation over night, the cultures were raised to the air medium interface by lowering the medium level. The medium was changed every second day. Cultures were harvested after 14 days, embedded in Tissue-Tek (Sakura, Zoeterwoude, The Netherlands) and frozen in liquid nitrogen.

Tissues

Samples of human skin, split skin, and human MM metastases were obtained in the course of routine pathological diagnoses from the Departments of Dermatology and Pathology of the Medical Center Mannheim. Samples were snap-frozen in isopentane, which had been precooled to −80°C in liquid nitrogen and stored at −80°C. Procedures were performed with approval of the medical ethical committee of the Medical Center Mannheim of the University of Heidelberg, with patients' informed consent and according to the Declaration of Helsinki Principles. For analyses of the cad profiles in melanoma metastases, immunolabelled cryostat sections were evaluated by two independent investigators with respect to the proportion of immunoreactive tumor cells. Metastases with 10–50% immunoreactive tumor cells were classified as "+", those with 50–75% reactive cells as "++", and those with ⩾75% as "+++" (Table 2).

Immunoblotting, IP, and matrix-assisted laser desorption ionization analyses

Immunoblotting was performed as described by Peitsch *et al.* (1999), using total protein lysates of cultured cells or of human skin. For IP, cells grown to confluency were lysed either in a Triton X-100 IP buffer, containing 1% Triton X-100, 150 mM NaCl, and 20 mM 4-(2-hydroxyethyl)-1-piperazineethanesulfonic acid (pH 7.4) or in a RIPA buffer composed of 1% Triton X-100, 0.1% SDS, 0.5% sodium desoxycholate, 1 mM dithiothreitol, 0.5 mM $CaCl_2$, 150 mM NaCl, and 20 mM 4-(2-hydroxyethyl)-1-piperazineethanesulfonic acid (pH 7.4), both supplemented with a protease-inhibitor cocktail (Complete

Mini Inhibitor Tabs, EDTA-free; Roche Diagnostics, Mannheim, Germany), for 1 hour on ice. The supernatants obtained after centrifugation at 14.000 r.p.m. for 10 minutes (4°C) were subjected to IP, using pan mouse IgG or sheep anti-rabbit IgG Dynabeads (Dynal, Hamburg, Germany; cf. Peitsch *et al.*, 1999, 2005). Trypsin digestion and matrix-assisted laser desorption ionization–time of flight analyses were conducted by Dr Martina Schnölzer and Dr Tore Kempf (Protein Analysis Facility, German Cancer Research Center), as previously reported (Peitsch *et al.*, 1999).

RNA isolation, cDNA synthesis, and PCR

Isolation of total RNA from cultured cells and human split skin was performed with TriPure Isolation Reagent (Roche Diagnostics), according to the manufacturer's instructions. Cultured cells were vigorously vortexed and pipetted up and down for homogenization; split skin was pulverized in a micro-dismembrator (Braun Biotech International, Melsungen, Germany). The final concentrations of RNA were determined in an Ultrospec 2100 pro spectrometer (GE Healthcare Life Sciences, formerly Amersham Biosciences, Buckinghamshire, England), and quality was checked on formaldehyde-containing 1% agarose gels. For long-term storage at −80°C, RNA was precipitated with 2.5 volumes ethanol and 0.1 volume 3 M sodium acetate (pH 5.2).

Synthesis of cDNA was conducted with 10 μg total RNA as template, using 0.6 mM dNTP , 0,75 μg random primer dT7, 40 U protector RNAse inhibitor, and 10 U AMV reverse transcriptase in 50 μl 1 × AMV reverse transcriptase buffer (Roche Diagnostics), at 41°C for 1 hour, 51°C for 30 minutes, and 92°C for 3 minutes. The cDNA samples were replenished to a volume of 1 ml with TE buffer. For PCR, aliquots of 5 μl cDNA were utilized together with 0.2 mM deoxyribonucleotide triphosphate, 100 ng of each oligonucleotide primer and 1 U TAQ DNA polymerase in 50 μl $MgCl_2$-containing PCR buffer (Roche Diagnostics). The reaction profile was as follows: 3 minutes 94°C (initial denaturation), 34 cycles at 94°C (20 seconds), 54°C (30 seconds), and 72°C (1 minute), followed by a final elongation step at 72°C for 10 minutes. PCRs were performed for human Dsg1 (forward primer: 5′-GCACTGGTACAATTAATATTAACA-3′; reverse primer: 5′-TCCC TGGGTTCAGGCTGTGGTCCT-3′), human Dsg2 (forward primer: 5′-GCCAAGAAAGTACCAGTGTGCTGC-3′; reverse primer: 5′-CTTT CATCGTGGCTTCCTTGGCCA-3′) and, for control, for the actin-binding protein drebrin (forward primer: 5′-TTTAGATCTGCCGGCGT CAGCTTCAGCGGC-3′; reverse primer: 5′-CGCACTTGCGGGCAT CAGGCACAT-3′). PCR fragments were analyzed on 2% agarose gels.

Immunofluorescence and confocal laser scanning microscopy

For immunostainings, cultured cells grown on glass coverslips were fixed in 2% formaldehyde for 5–7 minutes, treated with NH_4Cl for blocking of free aldehyde groups (5 minutes), washed in PBS (5 minutes), and permeabilized with 0.1% Triton-X (2–3 minutes), followed by two washes in PBS. Alternatively, fixation was performed for 5 minutes at −20°C in methanol and permeabilization for 20 seconds in acetone (−20°C). For staining of tissues and organotypic HaCaT–melanoma cell cultures, frozen samples were sectioned at 5 μm thickness, using a Jung CM3000 cryomicrotome (Leica Microsystems, Wetzlar, Germany), air-dried for a minimum of 1 hour and either fixed in 2% formaldehyde as described above or in acetone for 10 minutes at −20°C. Before incubation with the first antibody, sections were blocked with 5% goat serum for 20 minutes. Both on cultured cells and on cryostat sections, primary antibodies were applied for 1 hour at room temperature, followed by three washes in PBS (5 minutes each), incubation with the secondary antibody (30 minutes, room temperature), washing with PBS (3 × 5 minutes), a short rinse in distilled water, and dehydration in 100% ethanol (1 minute). After air-drying, specimens were mounted with Fluoromount-G (Southern Biotech, obtained through Biozol Diagnostica, Eching, Germany).

PKPs are dual localization proteins, facultatively accumulating not only in intercellular contacts but also in the nucleus (Mertens *et al.*, 1996). The latter localization can best be visualized with a special short staining method guaranteeing minimal loss of soluble proteins, which was applied for PKP staining in addition to the above-mentioned protocols (Schmidt *et al.*, 1999). After methanol/acetone fixation, cells were incubated with primary antibodies only for 15 minutes, washed only twice for 2 minutes, covered with the secondary antibodies for 15 minutes, and washed twice for 2 minutes before mounting.

Immunofluorescence microscopical images were recorded with an Axiophot II photomicroscope (Carl Zeiss, Jena, Germany) equipped with an AxioCam HR (Carl Zeiss), for confocal laser scanning microscopy a Zeiss LSM 519UV microscope was used.

Electron and immunoelectron microscopy

Electron and immunoelectron microscopy was accomplished essentially as described (Langbein *et al.*, 2002). Briefly, for conventional electron microscopy, cells grown on coverslips were fixed in 2.5% glutaraldehyde in 50 mM sodium cacodylate (pH 7.2) for 30 minutes and then washed thrice in the same buffer. Postfixation was performed with 2% OsO_4 (cacodylate buffer) for 2 hours, followed first by several washes in distilled water and then by heavy metal staining (0.5% uranylacetate) overnight at 4°C. After three washes in distilled water, samples were dehydrated through an ethanol series and in propylenoxide, followed by embedding in Epon. Ultrathin sections for electron microscopy (EM) were made with a Reichert-Jung microtome (Utracut, Leica, Bensheim, Germany). For contrast enhancement, the sections were stained with 2% uranylacetate in methanol for 15 minutes and with lead citrate for 5 minutes.

For immunoelectron microscopy, cells were fixed in 2% formaldehyde and permeabilized with 0.1% Triton X-100 as mentioned above. Primary antibodies were applied for 2 hours. Antibodies conjugated with 1.4-nm gold particles (Nanogold, Biotrend, Cologne, Germany) were used as secondary reagent and incubated for 4 hours. Postfixation and silver enhancement were performed as described (Langbein *et al.*, 2002). Electron micrographs were taken at 80 kV, using an EM 910 (Carl Zeiss).

CONFLICT OF INTEREST

The authors state no conflict of interest.

ACKNOWLEDGMENTS

We thank Dr Martina Schnölzer and Dr Tore Kempf (Protein Analysis Facility, German Cancer Research Center, Heidelberg) for performing the MALDI–TOF analyses. PD Dr Selma Ugurel, Dr Jörg Faulhaber, and Dr Wolfgang Koenen (Department of Dermatology, Medical Center Mannheim, University of Heidelberg) are acknowledged for providing frozen tissue samples of melanoma metastases and human split skin. We would also like to thank Jutta Bulkescher, Yvette Dörflinger, and Christel Herbst (Department of Dermatology, Medical Center Mannheim) for excellent technical assistance.

This work was supported by a grant from the Deutsche Forschungsgemeinschaft to W. K. Peitsch (project PE 896/1).

REFERENCES

Amagai M, Karpati S, Klaus-Kovtun V, Udey MC, Stanley JR (1994) Extracellular domain of pemphigus vulgaris antigen (desmoglein 3) mediates weak homophilic adhesion. *J Invest Dermatol* 103:609–15

Andersen K, Nesland JM, Holm R, Florenes VA, Fodstad O, Maelandsmo GM (2004) Expression of S100A4 combined with reduced E-cadherin expression predicts patient outcome in malignant melanoma. *Mod Pathol* 17:990–7

Bauer R, Hein R, Bosserhoff AK (2005) A secreted form of P-cadherin is expressed in malignant melanoma. *Exp Cell Res* 305:418–26

Bauer R, Wild PJ, Meyer S, Bataille F, Pauer A, Klinkhammer-Schalke M *et al.* (2006) Prognostic relevance of P-cadherin expression in melanocytic skin tumours analysed by high-throughput tissue microarrays. *J Clin Pathol* 59:699–705

Borrmann CM, Grund C, Kuhn C, Hofmann I, Pieperhoff S, Franke WW (2006) The *area composita* of adhering junctions connecting heart muscle cells of vertebrates.II. Colocalizations of desmosomal and fascia adhaerens molecules in the intercalated disk. *Eur J Cell Biol* 85:469–85

Boukamp P, Petrussevska RT, Breitkreutz D, Hornung J, Markham A, Fusenig NE (1988) Normal keratinization in a spontaneously immortalized aneuploid human keratinocyte cell line. *J Cell Biol* 106:761–71

Cavallaro U, Christofori G (2004) Multitasking in tumor progression: signaling functions of cell adhesion molecules. *Ann N Y Acad Sci* 1014:58–66

Chidgey MA, Clarke JP, Garrod DR (1996) Expression of full-length desmosomal glycoproteins (desmocollins) is not sufficient to confer strong adhesion on transfected L929 cells. *J Invest Dermatol* 106:689–95

Chitaev NA, Leube RE, Troyanovsky RB, Eshkind LG, Franke WW, Troyanovsky SM (1996) The binding of plakoglobin to desmosomal cadherins: patterns of binding sites and topogenic potential. *J Cell Biol* 133:359–69

Chitaev NA, Troyanovsky SM (1997) Direct Ca2+-dependent heterophilic interaction between desmosomal cadherins, desmoglein and desmocollin, contributes to cell-cell adhesion. *J Cell Biol* 138:193–201

Christofori G (2003) Changing neighbours, changing behaviour: cell adhesion molecule-mediated signalling during tumour progression. *EMBO J* 22:2318–23

Cowin P, Kapprell HP, Franke WW, Tamkun J, Hynes RO (1986) Plakoglobin: a protein common to different kinds of intercellular adhering junctions. *Cell* 46:1063–73

Danen EH, de Vries TJ, Morandini R, Ghanem GG, Ruiter DJ, van Muijen GN (1996) E-cadherin expression in human melanoma. *Melanoma Res* 6:127–31

Duguay D, Foty RA, Steinberg MS (2003) Cadherin-mediated cell adhesion and tissue segregation: qualitative and quantitative determinants. *Dev Biol* 253:309–23

Foty RA, Steinberg MS (2005) The differential adhesion hypothesis: a direct evaluation. *Dev Biol* 278:255–63

Franke WW, Borrmann CM, Grund C, Pieperhoff S (2006) The *area composita* of adhering junctions connecting heart muscle cells of vertebrates.I. Molecular definition in intercalated disks of cardiomyocytes by immunoelectron microscopy of desmosomal proteins. *Eur J Cell Biol* 85:69–82

Getsios S, Huen AC, Green KJ (2004) Working out the strength and flexibility of desmosomes. *Nat Rev Mol Cell Biol* 5:271–81

Haass NK, Smalley KS, Herlyn M (2004) The role of altered cell–cell communication in melanoma progression. *J Mol Histol* 35:309–18

Haass NK, Smalley KS, Li L, Herlyn M (2005) Adhesion, migration and communication in melanocytes and melanoma. *Pigment Cell Res* 18:150–9

Heid HW, Schmidt A, Zimbelmann R, Schäfer S, Winter-Simanowski S, Stumpp S *et al.* (1994) Cell type-specific desmosomal plaque proteins of the plakoglobin family: plakophilin 1 (band 6 protein). *Differentiation* 58:113–31

Hendrix MJ, Seftor EA, Meltzer PS, Gardner LM, Hess AR, Kirschmann DA *et al.* (2001) Expression and functional significance of VE-cadherin in aggressive human melanoma cells: role in vasculogenic mimicry. *Proc Natl Acad Sci USA* 98:8018–23

Hess AR, Seftor EA, Gruman LM, Kinch MS, Seftor RE, Hendrix MJ (2006) VE-cadherin regulates EphA2 in aggressive melanoma cells through a novel signaling pathway: implications for vasculogenic mimicry. *Cancer Biol Ther* 5:228–33

Hsu MY, Meier FE, Nesbit M, Hsu JY, Van Belle P, Elder DE *et al.* (2000) E-cadherin expression in melanoma cells restores keratinocyte-mediated growth control and down-regulates expression of invasion-related adhesion receptors. *Am J Pathol* 156:1515–25

Hsu MY, Wheelock MJ, Johnson KR, Herlyn M (1996) Shifts in cadherin profiles between human normal melanocytes and melanomas. *J Investig Dermatol Symp Proc* 1:188–94

Huber MA, Kraut N, Beug H (2005) Molecular requirements for epithelial mesenchymal transition during tumor progression. *Curr Opin Cell Biol* 17:548–58

Itoh M, Morita K, Tsukita S (1999) Characterization of ZO-2 as a MAGUK family member associated with tight as well as adherens junctions with a binding affinity to occludin and alpha catenin. *J Biol Chem* 274:5981–6

Itoh M, Nagafuchi A, Yonemura S, Kitani-Yasuda T, Tsukita S, Tsukita S (1993) The 220-kD protein colocalizing with cadherins in non-epithelial cells is identical to ZO-1, a tight junction-associated protein in epithelial cells: cDNA cloning and immunoelectron microscopy. *J Cell Biol* 121:491–502

Klingelhöfer J, Troyanovsky RB, Laur OY, Troyanovsky S (2000) Amino-terminal domain of classic cadherins determines the specificity of the adhesive interactions. *J Cell Sci* 113:2829–36

Koeser J, Troyanovsky SM, Grund C, Franke WW (2003) *De novo* formation of desmosomes in cultured cells upon transfection of genes encoding specific desmosomal components. *Exp Cell Res* 285:114–30

Kowalczyk AP, Borgwardt JE, Green KJ (1996) Analysis of desmosomal cadherin-adhesive function and stoichiometry of desmosomal cadherin-plakoglobin complexes. *J Invest Dermatol* 107:293–300

Kuphal S, Bosserhoff AK (2006) Influence of the cytoplasmic domain of E-cadherin on endogenous N-cadherin expression in malignant melanoma. *Oncogene* 25:248–59

Kuphal S, Poser I, Jobin C, Hellerbrand C, Bosserhoff AK (2004) Loss of E-cadherin leads to upregulation of NFkappaB activity in malignant melanoma. *Oncogene* 23:8509–19

Kurzen H, Moll I, Moll R, Schäfer S, Simics E, Amagai M *et al.* (1998) Compositionally different desmosomes in the various compartments of the human hair follicle. *Differentiation* 63:295–304

Lampugnani MG, Resnati M, Raiteri M, Pigott R, Pisacane A, Houen G *et al.* (1992) A novel endothelial-specific membrane protein is a marker of cell–cell contacts. *J Cell Biol* 118:1511–22

Langbein L, Grund C, Kuhn C, Praetzel S, Kartenbeck J, Brandner JM *et al.* (2002) Tight junctions and compositionally related junctional structures in mammalian stratified epithelia and cell cultures derived therefrom. *Eur J Cell Biol* 81:419–35

Le Douarin N (1984) Pigment cells. In: *The neural crest.* (Le Douarin N ed.) Cambridge, London, New York, New Rochelle, Melbourne, Sydney: Cambridge University Press, 108–33

Li G, Fukunaga M, Herlyn M (2004) Reversal of melanocytic malignancy by keratinocytes is an E-cadherin-mediated process overriding beta-catenin signaling. *Exp Cell Res* 297:142–51

Li G, Satyamoorthy K, Herlyn M (2001a) N-cadherin-mediated intercellular interactions promote survival and migration of melanoma cells. *Cancer Res* 61:3819–25

Li G, Schaider H, Satyamoorthy K, Hanakawa Y, Hashimoto K, Herlyn M (2001b) Downregulation of E-cadherin and Desmoglein 1 by autocrine hepatocyte growth factor during melanoma development. *Oncogene* 20:8125–35

Liu ZJ, Xiao M, Balint K, Smalley KS, Brafford P, Qiu R *et al.* (2006) Notch1 signaling promotes primary melanoma progression by activating mito-

gen-activated protein kinase/phosphatidylinositol 3-kinase-Akt pathways and up-regulating N-cadherin expression. *Cancer Res* 66:4182–90

Matsuyoshi N, Tanaka T, Toda K, Imamura S (1997) Identification of novel cadherins expressed in human melanoma cells. *J Invest Dermatol* 108:908–13

Mertens C, Kuhn C, Franke WW (1996) Plakophilins 2a and 2b: constitutive proteins of dual location in the karyoplasm and the desmosomal plaque. *J Cell Biol* 135:1009–25

Moll R, Cowin P, Kapprell HP, Franke WW (1986) Desmosomal proteins: new markers for identification and classification of tumors. *Lab Invest* 54:4–25

Niessen CM, Gumbiner BM (2002) Cadherin-mediated cell sorting not determined by binding or adhesion specificity. *J Cell Biol* 156:389–99

Nollet F, Kools P, van Roy F (2000) Phylogenetic analysis of the cadherin superfamily allows identification of six major subfamilies besides several solitary members. *J Mol Biol* 299:551–72

Nuber UA, Schäfer S, Stehr S, Rackwitz HR, Franke WW (1996) Patterns of desmocollin synthesis in human epithelia: immunolocalization of desmocollins 1 and 3 in special epithelia and in cultured cells. *Eur J Cell Biol* 71:1–13

Omelchenko T, Fetisova E, Ivanova O, Bonder EM, Feder H, Vasiliev JM *et al.* (2001) Contact interactions between epitheliocytes and fibroblasts: formation of heterotypic cadherin-containing adhesion sites is accompanied by local cytoskeletal reorganization. *Proc Natl Acad Sci USA* 98:8632–7

Onken MD, Ehlers JP, Worley LA, Makita J, Yokota Y, Harbour JW (2006) Functional gene expression analysis uncovers phenotypic switch in aggressive uveal melanomas. *Cancer Res* 66:4602–9

Paffenholz R, Kuhn C, Grund C, Stehr S, Franke WW (1999) The arm-repeat protein NPRAP (neurojungin) is a constituent of the plaques of the outer limiting zone in the retina, defining a novel type of adhering junction. *Exp Cell Res* 250:452–64

Patel SD, Chen CP, Bahna F, Honig B, Shapiro L (2003) Cadherin-mediated cell–cell adhesion: sticking together as a family. *Curr Opin Struct Biol* 13:690–8

Peitsch WK, Grund C, Kuhn C, Schnölzer M, Spring H, Schmelz M *et al.* (1999) Drebrin is a widespread actin-associating protein enriched at junctional plaques, defining a specific microfilament anchorage system in polar epithelial cells. *Eur J Cell Biol* 78:767–78

Peitsch WK, Hofmann I, Bulkescher J, Hergt M, Spring H, Bleyl U *et al.* (2005) Drebrin, an actin-binding, cell-type characteristic protein: induction and localization in epithelial skin tumors and cultured keratinocytes. *J Invest Dermatol* 125:761–74

Poser I, Dominguez D, de Herreros AG, Varnai A, Buettner R, Bosserhoff AK (2001) Loss of E-cadherin expression in melanoma cells involves up-regulation of the transcriptional repressor Snail. *J Biol Chem* 276:24661–6

Qi J, Chen N, Wang J, Siu CH (2005) Transendothelial migration of melanoma cells involves N-cadherin-mediated adhesion and activation of the beta-catenin signaling pathway. *Mol Biol Cell* 16:4386–97

Qi J, Wang J, Romanyuk O, Siu CH (2006) Involvement of Src family kinases in N-cadherin phosphorylation and beta-catenin dissociation during transendothelial migration of melanoma cells. *Mol Biol Cell* 17:1261–72

Qian X, Karpova T, Sheppard AM, McNally J, Lowy DR (2004) E-cadherin-mediated adhesion inhibits ligand-dependent activation of diverse receptor tyrosine kinases. *EMBO J* 23:1739–48

Robert G, Gaggioli C, Bailet O, Chavey C, Abbe P, Aberdam E *et al.* (2006) SPARC represses E-cadherin and induces mesenchymal transition during melanoma development. *Cancer Res* 66:7516–23

Sanders DS, Blessing K, Hassan GA, Bruton R, Marsden JR, Jankowski J (1999) Alterations in cadherin and catenin expression during the biological progression of melanocytic tumours. *Mol Pathol* 52:151–7

Sandig M, Voura EB, Kalnins VI, Siu CH (1997) Role of cadherins in the transendothelial migration of melanoma cells in culture. *Cell Motil Cytoskeleton* 38:351–64

Schäfer S, Koch PJ, Franke WW (1994) Identification of the ubiquitous human desmoglein, Dsg2, and the expression catalogue of the desmoglein subfamily of desmosomal cadherins. *Exp Cell Res* 211:391–9

Schmelz M, Duden R, Cowin P, Franke WW (1986) A constitutive transmembrane glycoprotein of Mr 165,000 (desmoglein) in epidermal and non-epidermal desmosomes.I. Biochemical identification of the polypeptide. *Eur J Cell Biol* 42:177–83

Schmidt A, Jäger S (2005) Plakophilins – hard work in the desmosome, recreation in the nucleus? *Eur J Cell Biol* 84:189–204

Schmidt A, Langbein L, Prätzel S, Rode M, Rackwitz HR, Franke WW (1999) Plakophilin 3 – a novel cell-type-specific desmosomal plaque protein. *Differentiation* 64:291–306

Shan WS, Tanaka H, Phillips GR, Arndt K, Yoshida M, Colman DR *et al.* (2000) Functional *cis*-heterodimers of N- and R-cadherins. *J Cell Biol* 148:579–90

Shimoyama Y, Tsujimoto G, Kitajima M, Natori M (2000) Identification of three human type-II classic cadherins and frequent heterophilic interactions between different subclasses of type-II classic cadherins. *Biochem J* 349:159–67

Silye R, Karayiannakis AJ, Syrigos KN, Poole S, van Noorden S, Batchelor W *et al.* (1998) E-cadherin/catenin complex in benign and malignant melanocytic lesions. *J Pathol* 186:350–5

Simonneau L, Kitagawa M, Suzuki S, Thiery JP (1995) Cadherin 11 expression marks the mesenchymal phenotype: towards new functions for cadherins? *Cell Adhes Commun* 3:115–30

Smalley KS, Brafford P, Haass NK, Brandner JM, Brown E, Herlyn M (2005) Up-regulated expression of zonula occludens protein-1 in human melanoma associates with N-cadherin and contributes to invasion and adhesion. *Am J Pathol* 166:1541–54

Stark HJ, Baur M, Breitkreutz D, Mirancea N, Fusenig NE (1999) Organotypic keratinocyte cocultures in defined medium with regular epidermal morphogenesis and differentiation. *J Invest Dermatol* 112: 681–91

Tang A, Eller MS, Hara M, Yaar M, Hirohashi S, Gilchrest BA (1994) E-cadherin is the major mediator of human melanocyte adhesion to keratinocytes *in vitro*. *J Cell Sci* 107:983–92

Tepass U, Truong K, Godt D, Ikura M, Peifer M (2000) Cadherins in embryonic and neural morphogenesis. *Nat Rev Mol Cell Biol* 1:91–100

Troyanovsky SM, Eshkind LG, Troyanovsky RB, Leube RE, Franke WW (1993) Contributions of cytoplasmic domains of desmosomal cadherins to desmosome assembly and intermediate filament anchorage. *Cell* 72: 561–74

Van Marck V, Stove C, Van Den Bossche K, Stove V, Paredes J, Vander Haeghen Y *et al.* (2005) P-cadherin promotes cell-cell adhesion and counteracts invasion in human melanoma. *Cancer Res* 65:8774–83

Volk T, Cohen O, Geiger B (1987) Formation of heterotypic adherens-type junctions between L-CAM-containing liver cells and A-CAM-containing lens cells. *Cell* 50:987–94

Wheelock MJ, Johnson KR (2003) Cadherins as modulators of cellular phenotype. *Annu Rev Cell Dev Biol* 19:207–35

Wuchter P, Boda-Heggemann J, Straub BK, Grund C, Kuhn C, Krause U *et al.* (2007) Processus and recessus adhaerentes: giant adherens cell junction systems connect and attract human mesenchymal stem cells. *Cell Tissue Res*, 20 March 2007 [E-pub ahead of print]